Evaluation of Global Horizontal Irradiance to Plane of Array Irradiance Models at Locations across the United States

Matthew Lave, *Member, IEEE,* William Hayes, Andrew Pohl, and Clifford W. Hansen

Abstract—We report an evaluation of the accuracy of combinations of models that estimate plane-of-array (POA) irradiance from measured global horizontal irradiance (GHI). This estimation involves two steps: (1) decomposition of GHI into direct and diffuse horizontal components; and (2) transposition of direct and diffuse horizontal irradiance to POA irradiance. Measured GHI and coincident measured POA irradiance from a variety of climates within the United States were used to evaluate combinations of decomposition and transposition models. A few locations also had diffuse horizontal irradiance (DHI) measurements, allowing for decoupled analysis of either the decomposition or the transposition models alone. Results suggest that decomposition models had mean bias differences (modeled versus measured) that vary with climate. Transposition model mean bias differences depended more on the model than the location. When only GHI measurements were available and combinations of decomposition and transposition models were considered, the smallest mean bias differences were typically found for combinations which included the Hay/Davies transposition model.

I. INTRODUCTION

MODELS which estimate plane-of-array (POA) irradiance from measured global horizontal irradiance (GHI) are critical to PV performance analysis because often only GHI measurements are available whereas the PV modules being analyzed are tilted to maximize annual energy production. Modeling POA irradiance from GHI involves two steps: (1) the decomposition of GHI into its direct and diffuse components, usually expressed as diffuse horizontal irradiance (DHI) and direct normal irradiance (DNI), and (2) the transposition of these components to POA of the modules. No combination of decomposition and transposition models is widely accepted as a standard for converting GHI to POA; various pairs of decomposition plus transposition models are in use. This lack of consistency leads to different predictions of POA irradiance, even when using the same input GHI. For example, Fig. 1 shows that annual POA energy estimated using the program PVsyst [1] can vary by over 1% simply by changing the transposition model from Hay/Davies [2] to Perez [3].
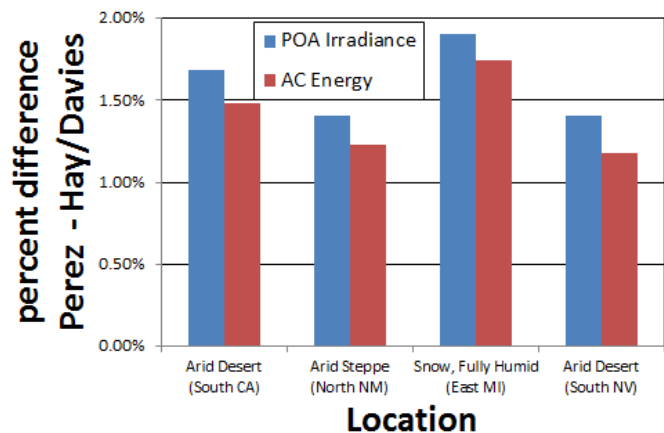

Fig. 1. Annual differences in POA irradiance and AC energy between the Perez and Hay/Davies transposition models as implemented in PVsyst.

There are numerous previous works evaluating either decomposition models (e.g., [4], [5]), transposition models (e.g., [6], [7], [8]), or combinations of both (e.g., [9]). However, most of these evaluations compare models with data at a single location (Ineichen [4] is a notable exception as 22 locations across the world were used to test decomposition models), and most do not go beyond simple annual metrics such as root mean squared error (RMSE) or mean bias error (MBE). Here, we evaluate the performance of decomposition models and transposition models separately, as well as combinations of decomposition with transposition models, at a variety of locations across the United States. Our work builds upon previous studies because we analyze each model's performance over many different test climates and we examine model performance in greater detail: we consider decomposition model errors as a function of clearness index, explore the impact of changing albedo, examine the relationship between the bias in model combinations and the biases in the separate decomposition and transposition models, and we use redundant sensors to reduce the effect of sensor measurement bias on the analysis.

M.Lave is with Sandia National Laboratories, Livermore, CA, 94550, USA (e-mail: mlave@sandia.gov).

W. Hayes is with First Solar, San Francisco, CA, 94105, USA.

A. Pohl and C. Hansen are with Sandia National Laboratories, Albuquerque, NM, 87185, USA.

II. MODELS

Figure 2 shows how a transposition model, or the combination of a decomposition and a transposition model, is used to estimate POA irradiance from available measurements. We discuss the specific models we considered in our analysis in the following subsections.

A. Decomposition Models

We considered the decomposition models listed in Table I. While this is not an exhaustive list of all decomposition models, it includes models that are commonly used (e.g., Erbs [10] which is used in PVSyst) or have been recently proposed as improvements over common models (e.g., Boland [11]). All models are empirical, in that their equations are not formally derived from physical laws but rather involve coefficients that were estimated from a fixed set of measured data at one or a handful of locations. We refer the reader to the references in Table I for detailed model descriptions.

Note that Reindl [12] proposes three different models of increasing complexity (termed here Reindl 1, Reindl 2, and Reindl 3) depending on the available input data. Additionally, it was found that the performance of the Reindl models during times of high clearness index might be improved by adjusting the bound between two of the piecewise clearness index intervals (see details in Appendix A). Specifically, in the Reindl adjusted models, the intervals in equations 2b, 3b, and 4b in [12] are changed to $0.3 < k_t < 0.83$ and the intervals in equations 2c, 3c, and 4c are changed to $0.83 < k_t$. The Reindl models with this adjustment are referred to here as the Reindl adjusted models.

TABLE I
DECOMPOSITION MODELS.

Model	Input variables (to compute DF)	Abbreviation
Orgill and Hollands [13]	Kt	OH
Erbs [10]	Kt	Er
Boland [11]	Kt	Bo
Reindl 1 [12]	Kt	R1
Reindl 1 adj	Kt	R1a
DISC [14]	$Kt, SunEl$	DIS
DIRINT [15]	$Kt, SunEl$	DIR
Reindl 2 [12]	$Kt, SunEl$	R2
Reindl 2 adj	$Kt, SunEl$	R2a
Reindl 3 [12]	$Kt, SunEl, AmbT, RH$	R3
Reindl 3 adj	$Kt, SunEl, AmbT, RH$	R3a
Posadillo [16]	$Kt, SunEl, MF$	Po

Most decomposition models compute the diffuse fraction, $DF = \frac{DHI}{GHI}$, which is then converted into DHI by multiplying by the GHI. Some models alternatively compute a direct fraction and hence DNI. Because DHI and DNI are related by:

$$DNI = \frac{GHI - DHI}{sin(SunEl)}, \quad (1)$$

all decomposition models effectively produce estimates of both DHI and DNI.

All decomposition models use at least the clearness index Kt to compute the diffuse fraction (or equivalent). Many models also account for the solar elevation angle $SunEl$.

The Reindl 3 models use the ambient temperature $AmbT$ and the relative humidity RH, while the Posadillo model uses a modulating function MF based on the 5-minute variability in GHI. DIRINT was used with its stability index, which is derived from the hour before, current, and hour after clearness index values.

B. Transposition Models

Table II lists the transposition models we evaluated. The Hay/Davies and Perez models are the most commonly used transposition models, while the Isotropic model gives a baseline with simple assumptions. The Sandia model is identical to the isotropic model, except that it uses an empirically-derived ground albedo (Eq. 5) instead of assuming a constant value. The transposition models determine total POA irradiance by estimating the direct, ground reflected diffuse, and sky diffuse components on the plane of array:

$$POA = POA_{dir} + POA_{diff,refl} + POA_{diff,sky}. \quad (2)$$

TABLE II
TRANSPOSITION MODELS.

Model	Input variables
Isotropic [17]	$SurfTilt, DHI$
Sandia (King) [18]	$SurfTilt, DHI, GHI, SunEl$
Hay/Davies [2]	$SurfTilt, SurfAz, DHI, DNI, HExtra, SunEl, SunAz$
Perez [3]	$SurfTilt, SurfAz, DHI, DNI, HExtra, SunEl, SunAz, AM$

In all models, the direct irradiance incident on the POA, POA_{dir}, is calculated directly from DNI through geometric relations:

$$POA_{dir} = DNI \times cos(AOI) \quad (3)$$

where AOI is the angle of incidence of the sun beam on the POA surface.

The ground reflected diffuse irradiance is estimated as a simple function of GHI, ground albedo (ρ), and the surface tilt from horizontal (β) by making the general assumptions of isotropic reflection and constant albedo in the field of view:

$$POA_{diff,refl} = GHI \times \rho \times \frac{1 - cos(\beta)}{2}. \quad (4)$$

All transposition models we consider use Eqn. 4. The Isotropic, Hay/Davies, and Perez models use a constant albedo; we assume $\rho = 0.2$ in this analysis (see section IV-D1 for a discussion of this assumption). The Sandia transposition model uses an albedo equation that was empirically fit to data from Albuquerque, NM:

$$\rho = 0.012 \times SunZen - 0.04, \quad (5)$$

where $SunZen$ is the solar zenith angle in degrees.

The transposition models vary in their estimation of the sky diffuse irradiance on the POA, $POA_{diff,sky}$. The Isotropic and Sandia models use an isotropic sky assumption such that the diffuse POA irradiance depends only on the amount of sky 'seen' by the surface. The Hay/Davies model separates the sky diffuse irradiance into two components – circumsolar diffuse
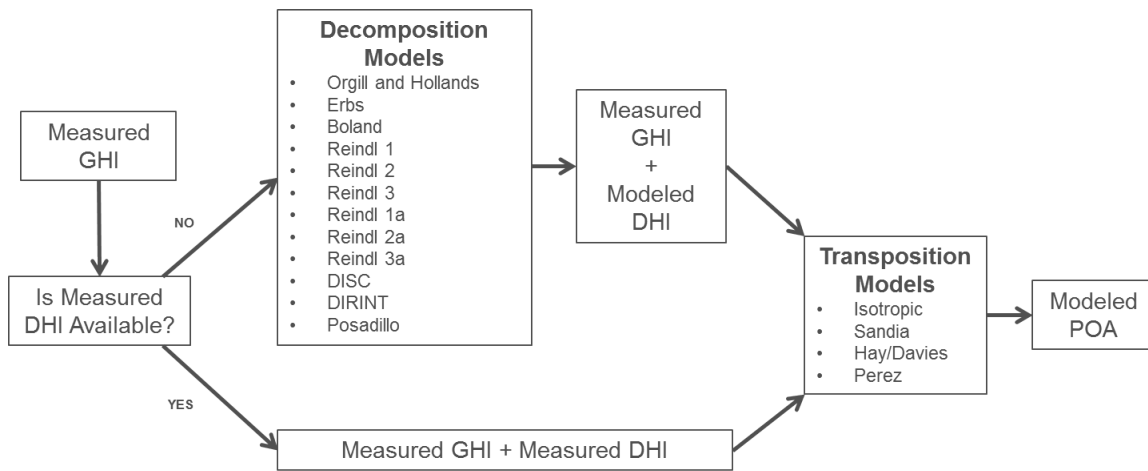
Fig. 2. Flowchart showing how to model POA irradiance from measured GHI.

irradiance which is a function of the angle of incidence (in the same form as direct irradiance is treated in Eq. 3) and rest-of-sky diffuse irradiance using the isotropic assumption – with an anisotropic index based on the amount of DNI relative to HExtra used to determine the fraction of the sky represented by each component. The Perez model separates the sky diffuse irradiance into three components – circumsolar, near-horizon, and rest-of-sky – with separate models and lookup tables of coefficients for each component and for weighting between components (see [3] for full details). The Perez model was implemented using the composite coefficients (derived by aggregating results from multiple locations) listed in [3].

III. Data Description

Details about the data at each location are shown in Table III, and the station locations are mapped in Fig. 3. Data for Stations 1-6 was contributed by First Solar, Inc., and GHI and POA measurements were taken using Kipp & Zonen CMP 11 secondary standard pyranometers (as defined in ISO 9060). Stations 3 and 4 also included DHI measurements using Irradiance, Inc. Rotating Shadowband Radiometers which rely on Licor LI-200 radiometers. The LI-200 radiometers have similar specifications as first class pyranometers [19]. Data for Station 9 was contributed by Southern Company, and LI-200 radiometers were used to measure GHI and POA irradiance. (Note that station numbering is not sequential due to the removal of two stations which did not have sufficient periods of record.) Station 10 is located in Golden, CO at NREL's Solar Radiation Research Laboratory [20]; the Global CM22 measurement from a secondary standard Kipp & Zonen CM22 was used for GHI, the Diffuse CM22 measurement from a CM22 with a diffuse shading disk was used for DHI, and the Global 40-South PSP measurement from a first class Eppley Precision Spectral Pyranometer (PSP) was used for POA irradiance. Stations 11 (Livermore, CA) and 12 (Albuquerque, NM) are operated by Sandia National Laboratories. Station 11 uses a PSP for GHI measurements and a PSP with a shadowband for DHI measurements, but does not have a POA measurement. Station 12 uses PSPs for GHI, DHI, and POA measurements (with a shadowband for the DHI measurement).
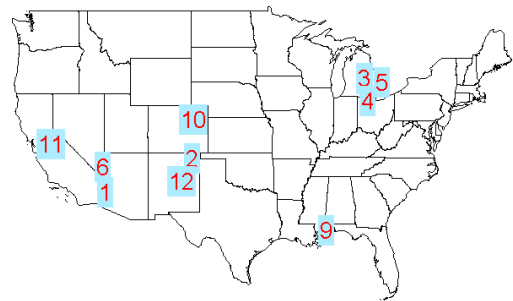

Fig. 3. Map of station locations.

For all stations except Station 9, data were available for one year or more. In these cases, we used only year-long periods of data (e.g., 1-year, 2-years, etc.) even though longer periods of record were available to ensure equal weighting of seasonal effects. At Station 9, only 10 months of data were available. We choose to include Station 9 in our analysis, but caution that winter effects may not be fully captured. All data were collected at a resolution of one minute. POA measurements were collected at due south azimuth, which is consistent with the majority of installed solar PV modules, but limits this analysis to south-oriented fixed tilt systems. Stations 2, 10, and 12 are at high altitude.

The stations equipped with DHI measurements (Stations 3, 4, 10, 11, 12) allowed for analysis of the decomposition models separately. The stations with both DHI and POA measurements (Stations 3, 4, 10, 12) allowed for separate analysis of the transposition models.

IV. Analysis

Three distinct analyses were undertaken: (A) decomposition models alone using measured GHI as input and compared to measured DHI, (B) transposition models alone using measured GHI and measured DHI as input and compared to measured POA, and (C) combinations of decomposition and transpo-

TABLE III
DATA LOCATIONS AND CLIMATES.

Station	Location	Elevation [m]	Climate Zone	Measured Data	Time Period	*SurfTilt*	*SurfAz*
1	Southeast CA	120	Arid Desert Hot (BWh)	GHI, POA	1/2010 - 12/2012	25°	180°
2	Northeast NM	1800	Arid Steppe Cold (BSk)	GHI, POA	1/2012 - 12/2012	25°	180°
3	East MI	188	Snow; Fully humid; Warm summer (Dfb)	GHI, DHI, POA	8/2012 - 7/2013	25°	180°
4	East MI	181	Snow; Fully humid; Warm summer (Dfb)	GHI, DHI, POA	8/2012 - 7/2013	25°	180°
5	East MI	193	Snow; Fully humid; Warm summer (Dfb)	GHI, POA	10/2010 - 9/2013	25°	180°
6	Southern NV	572	Arid Desert Hot (BWh)	GHI, POA	1/2011 - 12/2012	25°	180°
9	Coastal MS	6	Warm temperate; Fully humid; Hot summer (Cfa)	GHI, POA	2/2013 - 11/2013	15°	180°
10	Central CO	1829	Arid Steppe Cold (BSk)	GHI, DHI, POA	1/2013 -12/2013	40°	180°
11	Central CA	200	Warm temperate; dry, hot summer (CSa)	GHI, DHI	1/2013 -12/2013	N/A	N/A
12	Central NM	1657	Arid Steppe Cold (BSk)	GHI, DHI, POA	1/2011 12/2011	35°	180°

sition models using measured GHI as input and compared to measured POA. In this last case, DHI estimated from the decomposition models was input to the transposition models.

We first summarize all measured data to hourly averages because the considered models were designed to predict hourly values of their output quantities. Since errors in measurements may contribute to model errors in our analysis, we use the term "differences" rather than "errors" when comparing modeled to measured data, such that we report on root mean squared differences (RMSD) and mean bias differences (MBD). Measurement bias errors are difficult to distinguish from model bias errors, and may influence our analysis. We attempt to minimize the effect of measurement bias on our conclusions by evaluating the performance of the combined models using colocated pairs of GHI and POA sensors in section IV-D3.

Simple quality control metrics were applied to all data. All GHI, DHI, and POA values less than 0 Wm^{-2} or greater than 1300 Wm^{-2} were removed from the analysis, since these values were likely erroneous measurements. Additionally, any DHI measurement that exceeded the concurrent GHI measurement was set equal to the GHI measurement because it is not physically possible for DHI to exceed GHI. In these few situations, DHI only slightly exceeded GHI – the difference was not large enough to warrant rejecting the DHI measurement as erroneous. At the few times when POA measurements were excessively greater than GHI measurements (e.g., the POA measurement indicated clear-sky while the GHI measurement indicated overcast conditions), data were removed because the values were likely a result of data collection errors. Finally, hours for which the average extraterrestrial horizontal irradiance was less than 10 Wm^{-2} were eliminated from the analysis since they can lead to clearness index values much larger than the decomposition models were designed to accept. This led to discarding approximately 200 (varies by location) sunrise or sunset hours of data, but less than 0.01% of the total annual irradiation, so had a negligible effect on this analysis.

Specific quality control was needed at some of the locations. At one location, shading was observed that occluded the GHI sensor but not the POA sensor; times at which this shading occurred were eliminated from the analysis. At Stations 3 and 4, inconsistencies were found between the CMP11 measured GHI and the RSR/Licor measured GHI. We chose to use the CMP11 instrument because it is a higher standard (secondary standard), however, DHI measurements were only available from the RSR/Licor. Thus, we computed the diffuse fraction

($\frac{DHI_{RSR}}{GHI_{RSR}}$) using the RSR/Licor measurements, and then multiplied the CMP11-measured GHI by this diffuse fraction to obtain the DHI at Stations 3 and 4.

A. Decomposition Models

Relative accuracy of the decomposition models (modeled DHI compared to measured DHI) was evaluated for the five stations with DHI measurements (Stations 3, 4, 10, 11, and 12). Figure 4 shows the relative (% relative to GHI) Root Mean Squared Difference (rRMSD) and the relative Mean Bias Difference (rMBD) for each decomposition model and each station. These metrics quantify the average (over time) differences between modeled and measured data: rRMSD relates to the differences in hourly values and rMBD relates to the annual difference.
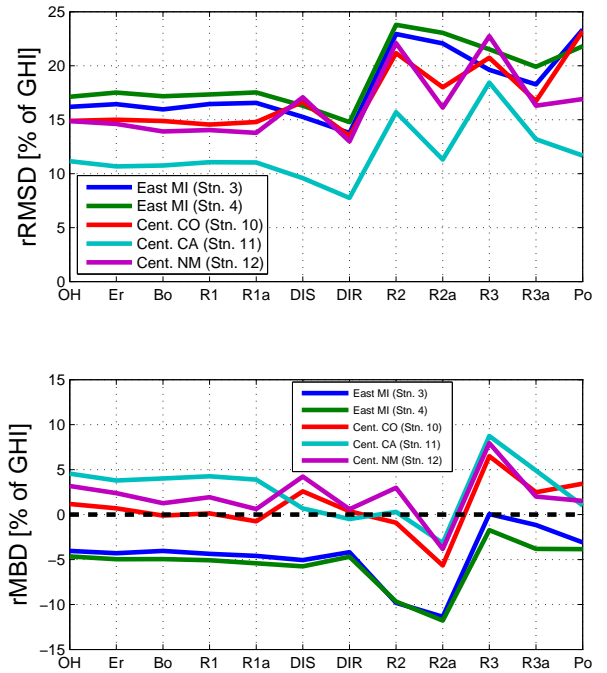

Fig. 4. Relative (to GHI) root mean squared (rRMSD) and mean bias (rMBD) differences (modeled minus measured) for each of the 12 decomposition models (x-axis) at each of the five stations with DHI measurements.

Model performance is similar across all stations for the "simple" decomposition models – those which only use Kt

and GHI as inputs (Orgill and Hollands, Erbs, Boland, Reindl 1, and Reindl 1a) – which have between 11-17% rRMSD. The rMBDs do not show this same consistency, as they range from -5% to +5% between stations, although at the same station all simple models have similar performance. Both the relative similarity of rRMSDs across locations and the variation of rMBD by location is in agreement with the findings of [4].

The rMBD differences by location were at least partly due to climate differences: the biases were negative for the cloudier eastern Michigan stations and were positive for the clearer Livermore and Albuquerque stations (again consistent with [4] who generally found negative bias errors in DNI models at clear locations). The simple decomposition models typically under-predict DHI during cloudy periods and over-predict DHI during clear periods.

Fig. 5 shows the errors in the Erbs model plotted as a function of the measured clearness index and diffuse fraction, and the rMBD as a function of clearness index. During partly cloudy periods, the Erbs model underestimates the DHI (dark colors in Fig. 5). The dominance of partly cloudy conditions at Station 3 (i.e., points falling above the black dashed line in Fig 5) causes a negative bias in the Erbs model. Conversely, during clear periods the Erbs model overestimates DHI (light colors in Fig. 5). At Station 11, the many clear periods (i.e., the collection of points around clearness index $Kt = 0.75$, diffuse fraction $DF = 0.1$) lead to a positive bias in the Erbs model.

Nearly identical bias trends were observed in all simple decomposition models. The more complicated decomposition models showed the same overall behavior – underestimating DHI in cloudy locations and overestimating DHI in clear locations – but bias analysis was more complicated due to the additional input variables used by the models.

At all locations, the DIRINT model had the smallest rRMSD and rMBD. However, the performance of the simple models was not significantly worse. Consequently, we focused our analysis of model combinations on those involving either the DIRINT model, because it shows the best performance, or the Erbs model, because it is representative of the simple models and is the default decomposition model in PVSyst.

B. Transposition Models

Using measured DHI values at Stations 3, 4, 10, and 12 the relative accuracy of the different transposition models was evaluated. Fig. 6 shows the rRMSDs and rMBDs.

With the exception of the Sandia model, the model biases were relatively consistent across the different locations. The isotropic model always produced the lowest POA estimates since it does not add any enhanced diffuse irradiance in the circumsolar region. The albedo correction that the Sandia model applies to the isotropic model caused the Sandia model to always have larger POA estimates than the isotropic model. Based on Eq. 5, the Sandia model albedo exceeds the 0.2 assumed in the isotropic model when the solar zenith angle is greater than $20°$, which almost always was the case at the stations considered due to their mid latitudes. The Sandia

model had the lowest rMBD at Station 12, as expected due to the model being calibrated using data at this location. rRMSDs were larger for the isotropic and Sandia models than for the Hay/Davies and Perez models.

Both the Hay/Davies and Perez models produced rMBDs that were smaller than 1.5% at all locations. The Perez model always estimated 1 to 2% more annual POA irradiance than the Hay/Davies model, consistent with the analysis run in PVsyst shown in Fig. 1. The Perez transposition model has the smallest rRMSD at all locations, indicating it may be the best model choice when measured DHI is available. However, the Hay/Davies model results in only slightly increased rRMSD. The magnitude of rRMSD values at Station 10 are consistent with those found in [9], which also used Station 10 for evaluation. However, the Perez rMBD was much more negative in [9] than found here. It is possible that different (e.g., location-specific) coefficients were used with the Perez model in [9], leading to this different result. Since the Perez and Hay/Davies models had the smallest rRMSD values and often had the smallest magnitude rMBD values, for combination models evaluation we focus on the Hay/Davies and Perez transposition models.

C. Combined Models

We focused our analysis on model combinations which involved the two best performing decomposition (Erbs and DIRINT) and transposition models (Hay/Davies and Perez), resulting in four combined models. The rRMSDs and rMBDs of these combined models are shown in Fig. 7.

The same order of transposition model rMBD (Perez > Hay/Davies) is observed. In the combined model case, however, all combinations tend to overestimate annual irradiance, meaning that combinations involving the Perez transposition model are now even more positively biased than noted in the transition model with measured DHI case. The DIRINT plus Hay/Davies model combination typically had the smallest rMBDs, though the Erbs plus Hay/Davies combination had only slightly larger rMBDs. The rRMSDs change more with changing station than with changing model. Although the rMBDs are rather consistent across Stations 2-6 ($\sim$1% for combinations involving Hay/Davies and $\sim$2% for combinations involving Perez), the rRMSDs vary widely across those locations (from <5% to over 10%).

D. Further Analysis of Combined Model Biases

This initial analysis of the combined models inspired three further investigations: (1) the impact of the assumption of albedo = 0.2 on combined model results, (2) how bias errors in measurements may be affecting combined model results, and (3) how the individual decomposition and transposition model biases related to the combined model biases.

1) Impact of Albedo Assumption: In Eq. 4, we assumed a ground albedo $\rho = 0.2$ for both the Hay/Davies and Perez transposition models. This is a simple assumption consistent with previous works (e.g., as used by [17] for snow-free months). However, Ineichen et al. [21] showed that this simple assumption may lead to large errors in ground reflected
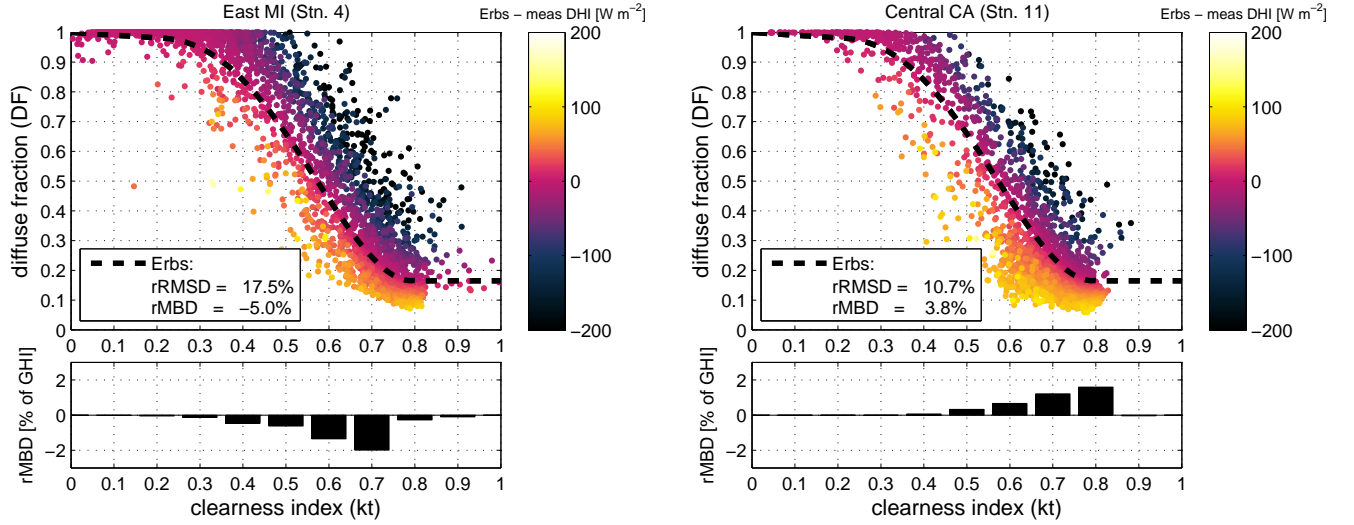
Fig. 5. [Top plots] Hourly differences (colors) in Erbs modeled minus measured DHI, plotted as a function of measured clearness index (x-axis) and measured diffuse fraction (y-axis). The black dashed line is the Erbs modeled diffuse fraction as a function of clearness index. [Bottom plots] Relative (to GHI) mean bias differences plotted as a function of clearness index.
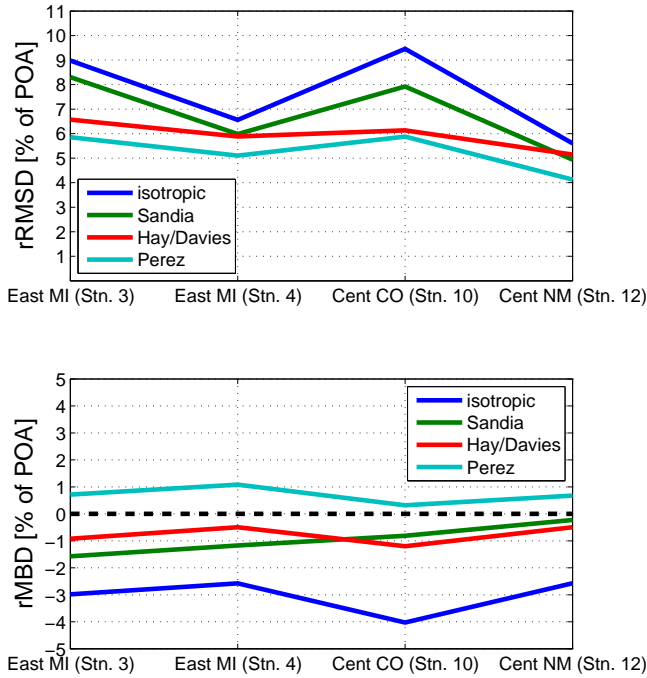

Fig. 6. Relative (to POA) root mean squared (RMSD) and mean bias (MBD) differences modeled versus measured for each of the 4 transposition models at each of the 4 stations with DHI and POA measurements.

diffuse estimates. To test the impact of varying albedo, we ran transposition and combined models with albedos ranging from 0.1 to 0.3. The rMBDs for the Hay/Davies and Perez transposition models, and the Erbs + Hay/Davies and Erbs + Perez combined models are shown in Fig. 8. Changing the albedo causes a larger change in rMBD at Stations 10 and 12 due to the high tilt angles (40° and 35°, respectively) and typically larger GHI values at these locations.

For the transposition models alone (dots in Fig. 8), in the $\rho = 0.2$ case the Hay/Davies and Perez models have similar magnitudes of rMBDs (as discussed in section IV-B). However, if the albedo were $\rho = 0.3$, the Perez model would have smaller rMBDs at all 4 test locations. Similarly, if $\rho = 0.1$, then the Hay/Davies model would have the smallest rMBDs. Since the true albedos are not known, we retain our conclusion (from section IV-B), that both the Hay/Davies and Perez models appear to have similar performance when using measured DHI.

For the combined models (lines in Fig. 8), at almost all station and albedo combinations, the Erbs + Hay/Davies model has the smallest rMBD. The only exceptions are for $\rho = 0.1$ at Stations 10 and 12, in which case the Erb + Perez model has the lowest rMBD. Because of the better performance by the Erbs + Hay/Davies model, we support the conclusion (from section IV-C) that when using modeled DHI, combined models including Hay/Davies appear to have the smallest rMBDs. This conclusion is consistent with Ineichen et al.'s [21] comment that the Perez model is highly sensitive to the quality of the measurements used, suggesting it may have weaker performance when inputting modeled DHI.

2) Possible Influence of Measurement Biases on Combined Model Findings: While it appears that model combinations involving Hay/Davies are less biased, our results could be influenced by sensor measurement biases. For example, if the POA measurement were biased high such that it recorded too much POA irradiance, even a perfect combined model (i.e., one that perfectly predicts the *true* POA) would be found to have a negative bias when compared to the biased measured POA. Similarly, a bias in the GHI measurement can affect the bias in the modeled POA irradiance.

We attempted to reduce the effect of sensor measurement bias by looking at multiple pairs of GHI and POA sensors at the same station. While each GHI or POA sensor may have
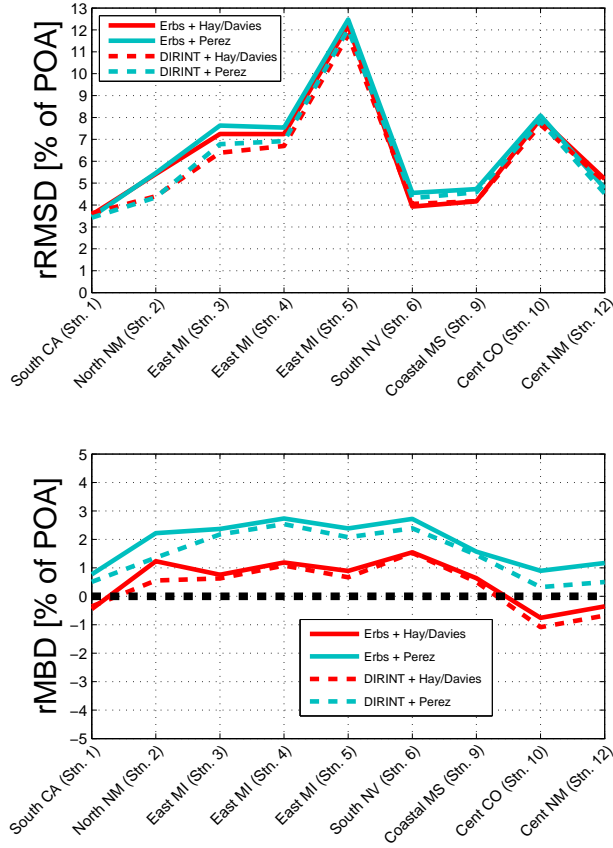
Fig. 7. Relative (to POA) root mean squared (rRMSD) and mean bias differences (rMBD) for combinations of decomposition and transposition models.
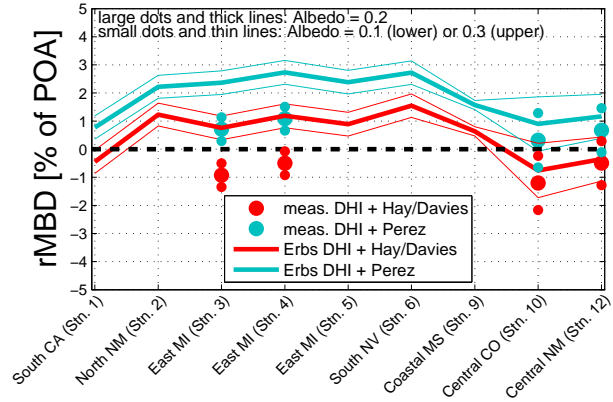

Fig. 8. Relative mean bias differences (rMBDs) when using measured DHI (dots) and when using Erbs modeled DHI (lines). The large dots and thick lines represent the $\rho = 0.2$ case (same as shown in Figs. 6 and 7). The small dots and thin lines represent the $\rho = 0.1$ (lower) and $\rho = 0.3$ (upper) cases.

a small measurement bias (e.g., due to calibration errors), we expect that the average bias over many pairs of GHI and POA sensors will be close to zero. Thus, by running the combined models for many different pairs of GHI and POA measurements, we will reduce the possible impact of measurement bias on our analysis. We focused on Stations 5 and 6 since they had the most pairs of GHI and POA sensors.

Station 5 had 6 GHI and 6 POA sensors (36 total possible GHI-POA sensor pairs), and Station 6 had 5 GHI and 5 POA sensors (25 total possible GHI-POA sensor pairs).
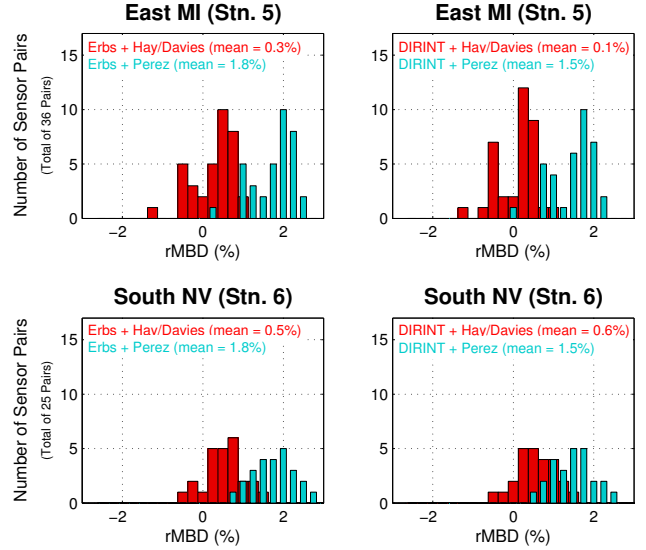

Fig. 9. Histogram of the counts in each rMBD bin (x-axis) for combined models using Erbs (left plots) or DIRINT (right plots) using the 36 (Stn. 5, top plots) or 25 (Stn. 6, bottom plots) possible combinations of GHI and POA sensors. For example, at Station 5 for the Erbs + Hay/Davies model (top left plot), there was one GHI-POA pair that resulted in a rMBD of -1.25%.

The distributions of rMBDs at Stations 5 and 6 for model combinations consisting of either Erbs or DIRINT plus Hay/Davies or Perez are shown in Fig 9. The widths of each distribution are around 3%, which is consistent with expected sensor uncertainties [22]. The mean rMBDs for combined models with Hay/Davies (0.2% to 0.5%) are always closer to zero than the mean rMBDs for models with Perez (1.4% to 1.7%). Thus, when sensor error is minimized, the model combinations with the Hay/Davies transposition model continue to show the smallest bias.

3) Relationship between Combined and Individual Model Biases: In the results shown in Fig. 7, the rMBDs at Stations 3 and 4 (cloudy locations) were more positive for the combined models than for the transposition models with measured DHI. This is expected since both the Erbs and DIRINT models underestimated DHI (Fig. 4), and when the decomposition models underestimate DHI, they inherently overestimate DNI (since DNI and DHI are related by Eq. 1). A larger DNI estimate then typically leads to a larger POA irradiance estimate since the POA is usually chosen to maximize direct (and hence annual) irradiance.

However, while both the Erbs and the DIRINT models had positive errors at Station 12 (+2.4% and +1.5%, respectively), suggesting a decrease in POA irradiance, the rMBD was practically unchanged for the combined models from the trans-position model with measured DHI case. The Erbs with Perez model actually leads to an increase in the POA irradiance.

Fig. 10 shows the relationship between decomposition model bias, transposition model bias, and combined model bias by plotting these rMBDs for all model combinations at Stations 3, 4, 10, and 12. It is expected that POA biases
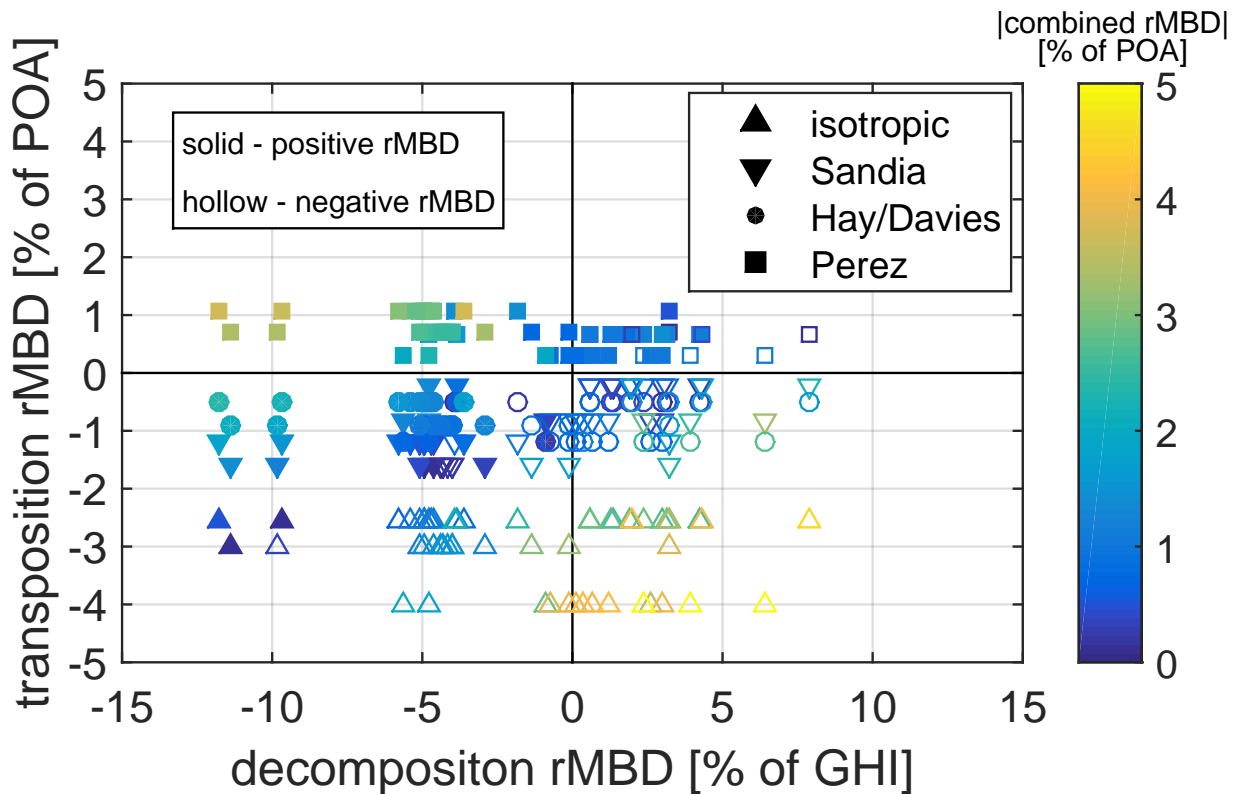
Fig. 10. Scatter plot of combined model rMBD plotted against the decomposition model (x-axis) and transposition model (y-axis) rMBDs. The combined model rMBD magnitudes are indicated by the colors (darker = closer to zero rMBD). Solid shapes indicated positive errors while hollow shapes indicated negative errors. All 12 decomposition models and all 4 transposition models evaluated at Stations 3, 4, 10, and 12 are included in this plot.

will increase moving to the left (decreasing DHI and hence increasing DNI estimates from decomposition models) and up (increasing POA estimates from the transposition models) in Fig. 10, and, indeed, for the most part this gradient was observed. However, some notable exceptions occur. Almost all model combinations involving the Perez transposition had positive biases, even when the decomposition models had positive biases. The isotropic model appears to be insensitive to small decomposition errors: model combinations including the isotropic model and a decomposition model with rMBD between -2% to +4% consistently had combined model rMBDs of -4% to -2.5%.

Deviations from the expected gradient (increasing combined model bias with decreasing decomposition model bias and increasing transposition model bias) are likely due to hourly deviations in the decomposition or transposition models which are not fully resolved with the rMBD metric. Due to the complicated dependencies of each model, biases in the decomposition models may be either minimized or amplified by the transposition models. Thus, biases in the individual models may suggest but do not necessarily determine the biases of the combined models. Based on the results shown in Figs. 7 and 10, combined models involving Hay/Davies appear to have less bias than combined models involving Perez, even though Hay/Davies and Perez had similar biases when using measured DHI.

V. CONCLUSION

Global horizontal irradiance (GHI) to plane of array (POA) irradiance models were evaluated at a variety of locations across the United States. Decomposition models had different biases based on location, consistent with previous findings [4]. This was caused by the models often underestimating the diffuse irradiance at cloudy locations and overestimating the diffuse at clear locations. Transposition model performance did not vary much by location; at all locations the isotropic model produced the smallest POA estimate and the Perez model the largest. Based on root mean squared deviation, the Erbs and DIRINT decomposition models and the Hay/Davies and Perez transposition models were chosen as the best performing models and used for evaluation of combined (decomposition plus transposition) model performance. Little difference was observed in the combined models whether DIRINT or Erbs was used for the decomposition model, but a large difference was seen between the model combinations involving the Hay/Davies versus the Perez transposition models. Model combinations involving the Hay/Davies transposition model appeared to have less bias than combinations involving the Perez transposition model, even though both Hay/Davies and Perez had similar bias magnitudes when using measured diffuse irradiance. Further analysis testing the impact of varying albedo, minimizing the effect of sensor measurement bias, and examining the impact of decomposition and transposition model bias on combined model bias continued to suggest

that combined models involving the Hay/Davies model led to smaller bias.

Currently, it is common for large, utility-scale PV plants to install one of more GHI sensors at the plant location before plant construction to obtain energy production estimates for financing. The combined model biases in transitioning from GHI to POA irradiance found here (often on the order of 1-3% even for the best model combinations) motivate additionally installing POA irradiance sensors to reduce errors in PV energy estimates.

Conversely, in locations where no ground measurements are available and modeled GHI (e.g., satellite-derived or TMY) is used, bias and random errors in the modeled GHI will contribute to errors in the final POA estimate (in addition to errors in the GHI to POA conversion). Further analysis is needed to understand how these modeled GHI errors interact with errors in the decomposition and transposition models.

While this work has suggested that it may be best to use the Hay/Davies model when measured diffuse irradiance is not available and a decomposition model is used to estimate diffuse irradiance, it also indicates that both decomposition and transposition models could be improved. Decomposition models could be modified to remove the locational dependence, possibly by using the clear-sky index which, as opposed to the clearness index, accounts for factors such as the atmospheric turbidity and station elevation. Further study of the circumsolar and other sky regions could enhance the transposition model performance. Transposition models could be designed to have less sensitivity to deviations in diffuse irradiance such that they have smaller biases when combined with decomposition models. Finally, transposition models were designed using fixed-tilt systems, but could be optimized for single- or two-axis tracking systems for broader application.

APPENDIX

A. Reindl Adjusted Models

The adjusted Reindl models were developed in previous (unpublished) analysis, motivated by the observation that empirically derived models, such as the Reindl models, have inaccuracies when used in climates that differ from the climate where they were developed.

This previous analysis used a limited dataset of measured GHI and measured DHI data collected at Station 2 (a short time period of DHI measurements were available at Station 2, but were not included in the main paper since a full year of data was not available). In comparing the Reindl modeled diffuse fraction to the measured diffuse fraction on an hourly basis, the Reindl model had poor performance at high clearness index values corresponding to the highest piecewise threshold of the model ($Kt \geq 0.78$), as shown in Fig. 11. There were many hours with large clearness index values, (e.g., $Kt \geq 0.78$) at Station 2 due to the low air mass at the high elevation. It was found for this dataset that an upper piecewise threshold of $Kt \geq 0.83$ led to a better fit of the measured data, motivating the adjusted Reindl models.

The adjusted Reindl models were included in the main paper to show the impact of slight modifications to existing
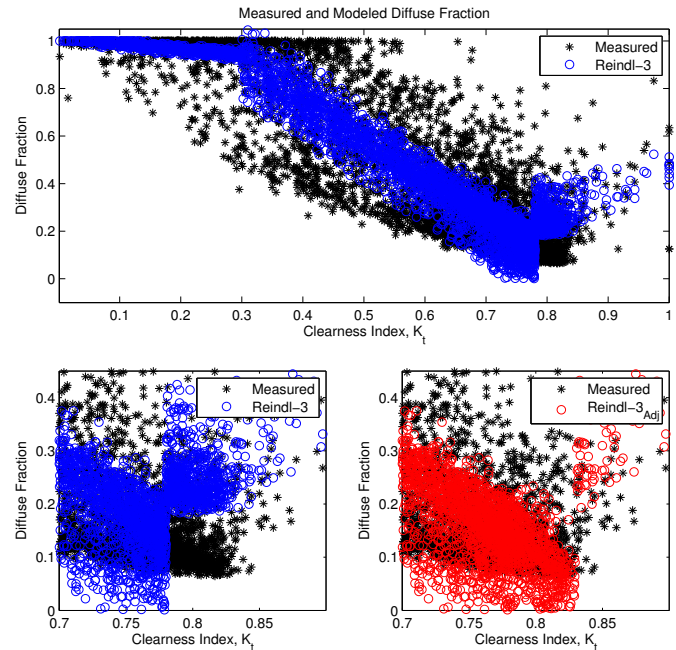

Fig. 11. Scatter plots of clearness index (x-axis) vs. diffuse fraction (y-axis) for (top) all clearness index values and (left and right) zoomed in on high clearness index values. In all plots, the black crosses show the measured diffuse fraction, the blue circles are the Reindl 3 modeled diffuse fraction, and the red circles are the Reindl 3 adjusted modeled diffuse fraction.

models. The Reindl 2 adjusted and Reindl 3 adjusted models were found to have smaller rRMSEs than the unadjusted models, especially at high-altitude (Stations 10 and 12) and predominantly clear (Station 11) locations (Fig. 4), showing an improvement when using the adjusted models. However, the Reindl adjusted models continue to have similar (Reindl 1 adjusted) or worse (Reindl 2 adjusted and Reindl 3 adjusted) performance than other decomposition models. This suggests that future model development should focus on developing accurate model forms rather than tweaking specific model parameters.

ACKNOWLEDGMENT

REFERENCES

[1] A. Mermoud, "PVsyst," http://www.pvsyst.com/.

[2] J. Hay and J. Davies, "Calculations of the solar radiation incident on an inclined surface," in *Proc. of First Canadian Solar Radiation Data Workshop, 59*. Ministry of Supply and Services, Canada, 1980.

[3] R. Perez, P. Ineichen, R. Seals, J. Michalsky, and R. Stewart, "Modeling daylight availability and irradiance components from direct and global irradiance," *Solar Energy*, vol. 44, no. 5, pp. 271–289, 1990.

[4] P. Ineichen, "Comparison and validation of three global-to-beam irradiance models against ground measurements," *Solar Energy*, vol. 82, no. 6, pp. 501 – 512, 2008. [Online]. Available: http://www.sciencedirect.com/science/article/pii/S0038092X07002551

[5] C. Jacovides, F. Tymvios, V. Assimakopoulos, and N. Kaltsounides, "Comparative study of various correlations in estimating hourly diffuse fraction of global solar radiation," *Renewable Energy*, vol. 31, no. 15, pp. 2492 – 2504, 2006. [Online]. Available: http://www.sciencedirect.com/science/article/pii/S0960148105003538

[6] P. G. Loutzenhiser, H. Manz, C. Felsmann, P. A. Strachan, T. Frank, and G. M. Maxwell, "Empirical validation of models to compute solar irradiance on inclined surfaces for building energy simulation," *Solar Energy*, vol. 81, no. 2, pp. 254–267, 2007.

[7] D. Wlodarczyk and H. Nowak, "Statistical analysis of solar radiation models onto inclined planes for climatic conditions of lower silesia in poland," *Archives of Civil and Mechanical Engineering*, vol. 9, no. 2, pp. 127 – 144, 2009. [Online]. Available: http://www.sciencedirect.com/science/article/pii/S1644966512600648

[8] A. M. Noorian, I. Moradi, and G. A. Kamali, "Evaluation of 12 models to estimate hourly diffuse irradiation on inclined surfaces," *Renewable Energy*, vol. 33, no. 6, pp. 1406 – 1412, 2008. [Online]. Available: http://www.sciencedirect.com/science/article/pii/S0960148107002509

[9] C. A. Gueymard, "Direct and indirect uncertainties in the prediction of tilted irradiance for solar engineering applications," *Solar Energy*, vol. 83, no. 3, pp. 432 – 444, 2009. [Online]. Available: http://www.sciencedirect.com/science/article/pii/S0038092X08002983

[10] D. G. Erbs, S. A. Klein, and J. A. Duffie, "Estimation of the diffuse radiation fraction for hourly, daily and monthly-average global radiation," *Solar Energy*, vol. 28, no. 4, pp. 293–302, 1982.

[11] J. Boland, B. Ridley, and B. Brown, "Models of diffuse solar radiation," *Renewable Energy*, vol. 33, no. 4, pp. 575–584, 2008.

[12] D. T. Reindl, W. A. Beckman, and J. A. Duffie, "Diffuse fraction correlations," *Solar Energy*, vol. 45, no. 1, pp. 1–7, 1990.

[13] J. F. Orgill and K. G. T. Hollands, "Correlation equation for hourly diffuse radiation on a horizontal surface," *Solar Energy*, vol. 19, no. 4, pp. 357–359, 1977.

[14] E. L. Maxwell, "A quasi-physical model for converting hourly global horizontal to direct normal insolation," Solar Energy Research Institute, Tech. Rep., 1987.

[15] R. Perez, "Dynamic global to direct conversion models," *ASHRAE Transactions Research Series*, pp. 154–168, 1992.

[16] R. Posadillo and R. López Luque, "Hourly distributions of the diffuse fraction of global solar irradiation in crdoba (spain)," *Energy Conversion and Management*, vol. 50, no. 2, pp. 223–231, 2009.

[17] B. Y. H. Liu and R. C. Jordan, "The interrelationship and characteristic distribution of direct, diffuse and total solar radiation," *Solar Energy*, vol. 4, no. 3, pp. 1–19, 1960.

[18] D. King, "Simple sandia sky diffuse model." [Online]. Available: http://pvpmc.org/modeling-steps/incident-irradiance/plane-of-array-poa-irradiance/calculating-poa-irradiance/poa-sky-diffuse/simple-sandia-sky-diffuse-model/

[19] LI-COR Environmental. (2014) Li-200 pyranometer specification. [Online]. Available: http://www.licor.com/env/products/light/pyranometers/200specs.html

[20] National Renewable Energy Laboratory, "Measurement and instrumentation data center." [Online]. Available: http://www.nrel.gov/midc

[21] P. Ineichen, R. Perez, and R. Seals, "The importance of correct albedo determination for adequately modeling energy received by tilted surfaces," *Solar Energy*, vol. 39, no. 4, pp. 301 – 305, 1987. [Online]. Available: http://www.sciencedirect.com/science/article/pii/S0038092X87800166

[22] T. Stoffel, "A review of measured/modeled solar resource uncertainty," in *2013 Sandia PV Performance Modeling Workshop*, 2013.

Matthew Lave received the Ph.D. degree in aerospace engineering from the University of California, San Diego.

He is a Senior Member of the Technical Staff at Sandia National Laboratories, working in the Photovoltaic and Distributed Systems Integration Department. His specialty areas are solar resource assessment, PV performance monitoring, and grid integration of PV, especially related to large data set analysis. He currently develops and validates models of solar irradiance, spatial smoothing of solar variability across large PV plants, and the impact of PV to the electric grid.

William Hayes received the M.S. degree in mechanical engineering from the University of California, San Diego.

He is a member of the Performance and Prediction team at First Solar, Inc. His expertise lies in modeling the thermal response of operational PV modules in utility scale deployment. He currently models and evaluates the performance of utility scale PV system focusing on driving down the uncertainty in PV system energy estimates.

Andrew Pohl received the B.S. degree in applied mathematics from the University of New Mexico and is currently pursuing the M.S. degree in statistics also from the University of New Mexico.

He is a student intern at Sandia National Laboratories, working in the Photovoltaic and Distributed System Integration Department.

Clifford W. Hansen received the Ph.D. degree in mathematics from The George Washington University in Washington, D.C.

He is a Distinguished Member of the Technical Staff at Sandia National Laboratories, working in the Photovoltaics and Distributed Systems Integration Department. His research focuses on methods for PV system modeling, model calibration from component characterization, and uncertainty in estimates of the solar resource and PV system production.